

Biomolecular events in cancer revealed by attractor metagenes

Wei-Yi Cheng¹ & Dimitris Anastassiou¹

Mining gene expression profiles has proven valuable for identifying metagenes, defined as linear combinations of individual genes, serving as surrogates of biological phenotypes. Typically, such metagenes are jointly generated as the result of an optimization process for dimensionality reduction. Here we present an unconstrained method for individually generating metagenes that can point to the core of the underlying biological mechanisms. We use an iterative process that starts from any seed gene and converges to one of several precise attractor metagenes representing biomolecular events, such as cell transdifferentiation or the presence of an amplicon. By analyzing six rich gene expression datasets from three different cancer types, we identified many such biomolecular events, some of which are present in all tested cancer types. We focus on several such events including a stage-associated mesenchymal transition and a grade-associated mitotic chromosomal instability.

Rich biomolecular datasets, publicly available at an increasing rate from sources such as The Cancer Genome Atlas (TCGA), provide unique opportunities for biological discovery from purely computational analysis. Gene expression signatures resulting from analysis of cancer datasets can serve as surrogates of cancer phenotypes¹. Subtypes in many cancer types²⁻⁴ have been identified by gene expression analysis often using techniques such as nonnegative matrix factorization⁵ combined with consensus clustering⁶.

The main objective addressed by techniques such as nonnegative matrix factorization is to reduce dimensionality by identifying a number of metagenes jointly representing the gene expression dataset as accurately as possible, in lieu of the whole set of individual genes. Each metagene is defined as a positive linear combination of the individual genes, so that its expression level is an accordingly weighted average of the expression levels of the individual genes. The identity of each resulting metagene is influenced by the presence of other metagenes within the objective of overall dimensionality reduction achieved by joint optimization.

In contrast, if the aim is not dimensionality reduction or classification into subtypes, but instead the independent and unconstrained identification of metagenes as surrogates of pure biomolecular events, then a different algorithm should be devised.

¹ Center for Computational Biology and Bioinformatics and Department of Electrical Engineering, Columbia University, 1312 S.W. Mudd Building, Mail Code 4712, 500 West 1120th Street, New York, NY 10027, USA. Correspondence should be addressed to D. Anastassiou (anastas@ee.columbia.edu)

This approach is devoid of cross-interference or mutual exclusivity requirements and has the advantage of increasing the chance of precisely identifying the particular genes at the core of the underlying biological mechanism as those that have the highest weights in the corresponding metagene, thus shedding more light on that mechanism. We found that, given a rich dataset represented by a gene expression matrix, such surrogate metagenes can be naturally identified as stable and precise attractors using a simple iterative approach. This identification is totally unsupervised, as it does not make use of any phenotypic association. Once identified, however, a metagene attractor is likely to be found associated with a phenotype.

We found that several attractor metagenes are present in nearly identical form in multiple cancer types. This provides an additional opportunity to combine the powers of a large number of rich datasets to focus, at an even sharper level, on the core genes of the underlying mechanism. For example, this methodology can precisely point to the causal (driver) oncogenes within amplicons to be among very few candidate genes. Importantly, this can be done from rich gene expression data, which already exist in abundance, without making any use of sequencing data.

We identified many attractors, which can directly lead to corresponding testable biological hypotheses. For the purposes of this paper we present the general methodology for the benefit of the research community together with a listing of the attractors in six datasets from three cancer types (ovarian, colon, breast). We also identified other attractors in other cancer types, such as leukemia, consistent with known facts about the nature of each disease. Here, we only focus on a few interesting cancer-associated attractors that we found present in these three solid cancer types.

RESULTS

Derivation of Attractor Metagenes

Given a nonnegative measure $J(G_i, G_j)$ of pairwise association between genes G_i and G_j , we define an attractor metagene $M = \sum_i w_i G_i$ to be a linear combination of the individual genes with weights $w_i = J(G_i, M)$. The association measure J is assumed to have minimum possible value 0 and maximum possible value 1, so the same is true for the weights. It is also assumed to be scale-invariant, therefore it is not necessary for the weights to be normalized so that they add to 1, and the metagenes can still be thought of as expressing a normalized weighted average of the expression levels of the individual genes.

According to this definition, the genes with the highest weights in an attractor metagene will have the highest association with the metagene (and, by implication, they will tend to be highly associated among themselves) and so they will often represent a biomolecular event reflected by the co-expression of these top genes. This can happen, e.g., when a biological mechanism is activated, or when a copy number variation (CNV), such as an amplicon, is present, in some of the samples included in the expression matrix. In the following we use the term “attractor” for simplicity to refer to

an attractor metagene, and the term “top genes” to refer to the genes with the highest weights in the attractor.

The definition of an attractor metagene can readily be generalized to include features other than gene expression, such as methylation values. It can also be used in datasets of any objects (not necessarily genes) characterized by any type of feature vectors, with applications in other disciplines, such as social and economic sciences.

The computational problem of identifying attractor metagenes given an expression matrix can be addressed heuristically using a simple iterative process: Starting from a particular seed (or “attractee”) metagene M , a new metagene is defined in which the new weights are $w_i = J(G_i, M)$. The same process is then repeated in the next iteration resulting in a new set of weights, and so forth. In all gene expression datasets that we tried we found that this process converges to a limited number of stable attractors. Each attractor is defined by a precise set of weights, which are reached with high accuracy typically within 10 or 20 iterations.

This algorithmic behavior with nice convergence properties is not surprising, because if a metagene contains some co-expressed genes with high weights, then the next iteration will naturally “attract” even more genes with the same properties, and so forth, until the process will eventually converge to a metagene representing a potential underlying biological event reflected by this co-expression. Furthermore, the set of the few genes with the highest weight are likely to represent the “heart” (core) of the biomolecular event. In support of this concept, the association of any of the top-ranked individual genes with the attractor metagene is consistently and significantly higher than the pairwise association between any of these genes, suggesting that the set of these top genes jointly comprise a proxy representing a biomolecular event better than each of the individual genes would. The top genes in the attractors can also serve as readily derived modules and we can use them in a complementary manner within the context of methods of identifying regulatory modules or other related approaches⁷.

Indeed, related versions of the signatures identified by attractors in this paper have been previously identified in various contexts, often intermingled with additional genes that may be unrelated or weakly related to the main underlying mechanism. However, the contribution of our work is that these signatures are recognized as multi-cancer biomolecular events, sharply pointing to the underlying mechanism. Therefore the top genes of the attractors will be appropriate for being used as biomarkers or for understanding the underlying biology. For example, one of the attractors that we identified (the “mitotic CIN” attractor, described below) has previously been found among sets of genes described generally⁸ as “proliferation” or “cell cycle related” markers, while the actual attractor points much more sharply to particular elements in the structure of the kinetochore.

A reasonable implementation of an “exhaustive” search is to only consider the seed metagenes in which one selected “attractee” gene is assigned a weight of 1 and all the other genes are assigned a weight of 0. The metagene resulting from the next iteration will then assign high weights to all genes highly associated with the originally

selected gene, to which we refer as the “attractee gene.” In this way all attractors representing biomolecular events characterized by coordinately co-expressed genes will be identified when these genes are used as attractees. The computational implementation of the algorithm is described in Online Methods. We note that a dual method can be used to identify attractor “metasamples” as representatives of subtypes, and we can also combine such metasamples with the attractor metagenes in various ways to achieve biclustering, but this topic is not examined in this paper.

We analyzed six datasets, two from ovarian cancer, two from breast cancer and two from colon cancer:

Dataset	Sample Size	Platform
Breast Wang (GSE2034)	286	Affymetrix HG-U133A
Breast TCGA	536	Agilent 244K Custom Gene Expression G4502A-07-3
Colon Jorrison (GSE14333)	290	Affymetrix HG-U133Plus 2.0
Colon TCGA	154	Agilent 244K Custom Gene Expression G4502A-07-3
Ovarian Tothill (GSE9891)	285	Affymetrix HG-U133Plus 2.0
Ovarian TCGA	584	Affymetrix HG-U133A

In each case, we identified general and genomically localized attractors and we found that many among them appear in similar forms in all six datasets. Following are descriptions of some of our results, starting with the three strongest multi-cancer attractors.

Mesenchymal Transition Attractor

This attractor contains mostly epithelial-mesenchymal transition (EMT)-associated genes. Table 1 provides a listing of top 100 genes based on their average mutual information (Online Methods) with their corresponding attractor metagenes.

This is a stage-associated attractor, in which the signature is significantly present only when a particular level of invasive stage, specific to each cancer type, has been reached. For example, this association can be demonstrated in three cancer datasets from different types (breast GSE3893, ovarian TCGA and colon GSE14333) that were annotated with clinical staging information: We can create a listing of differentially expressed genes, ranked by fold change, when ductal carcinoma in situ (DCIS) progresses to invasive ductal carcinoma; ovarian cancer progresses to stage III; and colon cancer progresses to stage II. In all three cases, the attractor is highly enriched among the top genes. Specifically, among the top 100 differentially expressed genes, the number of attractor genes included in Table 1 is 55 in breast cancer, 45 in ovarian cancer and 31 in colon cancer. The corresponding P values are 3×10^{-109} , 9×10^{-83} and 5×10^{-62} , respectively.

This attractor has been previously identified with remarkable accuracy as representing a particular kind of mesenchymal transition of cancer cells present in all types of solid cancers tested leading to a published list of top 64 genes^{9, 10}. Indeed 56 of these top 64 genes also appear in Table 1 ($P < 10^{-127}$), and furthermore all top 24 genes of Table 1 are among the 64. We found that most of the genes of the signature were expressed by the cancer cells themselves, and not by the surrounding stroma, at least in a neuroblastoma xenograft model that we tried¹⁰. We also found that the signature is associated with prolonged time to recurrence in glioblastoma¹¹. Related versions of the same signature were previously found to be associated with resistance to neoadjuvant therapy in breast cancer¹². These results are consistent with the finding that EMT induces cancer cells to acquire stem cell properties¹³. It has been hypothesized that EMT is a key mechanism for cancer cell invasiveness and motility¹⁴⁻¹⁶. The attractor, however, appears to represent a more general phenomenon of transdifferentiation present even in nonepithelial cancers such as neuroblastoma, glioblastoma and Ewing's sarcoma.

Although similar signatures are often labeled as “stromal,” because they contain many stromal markers such as α -SMA and fibroblast activation protein, the fact that most of the genes of the signature were expressed by xenografted cancer cells¹⁰, and not by mouse stromal cells, suggests that this particular attractor of coordinately expressed genes represents cancer cells having undergone a mesenchymal transition. The signature may indicate a non-fibroblastic transition, as occurs in glioblastoma, in which case collagen *COL1A1* is not co-expressed with the other genes of the attractor. We have hypothesized that a full fibroblastic transition of the cancer cells occurs when cancer cells encounter adipocytes¹⁰, in which case they may well assume the duties of cancer-associated fibroblasts (CAFs) in some tumors¹⁷. In that case, the best proxy of the signature⁹ is *COL1A1* and the strongly co-expressed genes *THBS2* and *INHBA*. Indeed, the 64 genes of the previously identified signature were found from multi-cancer analysis⁹ as the genes whose expression is consistently most associated with that of *COL1A1*.

The only EMT-inducing transcription factor found upregulated in the xenograft model¹⁰ is *SNAI2* (Slug), and it is also the one most associated with the signature in publicly available datasets. We also found that the microRNAs most highly associated with this attractor are miR-214, miR-199a, and miR-199b. Interestingly, miR-214 and miR-199a were found to be jointly regulated by another EMT-inducing transcription factor, *TWIST1*¹⁸.

Mitotic CIN Attractor

This attractor contains mostly kinetochore-associated genes. Table 2 provides a listing of the top 100 genes based on their average mutual information with their corresponding attractor metagenes, starting from *CENPA*, which encodes for a histone H3-like centromeric protein.

Contrary to the stage-associated mesenchymal transition attractor, this is a grade-associated attractor, in which the signature is significantly present only when an

intermediate level of tumor grade is reached. For example, this association can be demonstrated in three cancer datasets from different types (breast GSE3494, ovarian TCGA and bladder GSE13507) that were annotated with tumor grade information. We can create a listing of differentially expressed genes, ranked by fold change, when grade G2 is reached. In all three cases, the attractor is highly enriched among the top genes. Specifically, among the top 100 differentially expressed genes, the number of attractor genes included Table 2 is 41 in breast cancer, 36 in ovarian cancer and 26 in colon cancer. The corresponding P values are 7×10^{-73} , 4×10^{-61} and 5×10^{-47} , respectively. Consistently, a similar “gene expression grade index” signature¹⁹ was previously found differentially expressed between histologic grade 3 and histologic grade 1 breast cancer samples. Furthermore, that same signature¹⁹ was found capable of reclassifying patients with histologic grade 2 tumors into two groups with high versus low risks of recurrence.

This attractor is associated with chromosomal instability (CIN), as evidenced from the fact that another similar gene set comprising a “signature of chromosomal instability”²⁰ was previously derived from multiple cancer datasets purely by identifying the genes that are most correlated with a measure of aneuploidy in tumor samples. This led to a 70-gene signature referred to as “CIN70.” Indeed 34 of these 70 genes appear in Table 2 ($P < 10^{-61}$). However, several top genes of the attractor, such as *CENPA*, *KIF2C*, *BUB1* and *CCNA2* are not present in the CIN70 list. Mitotic CIN is increasingly recognized²¹ as a widespread multi-cancer phenomenon.

The attractor is characterized by overexpression of kinetochore-associated genes, which is known²² to induce CIN for reasons that are not clear. Overexpression of several of the genes of the attractor, such as the top gene *CENPA*²³, as well as *MAD2L1*²⁴ and *TPX2*²⁵, has also been independently previously found associated with CIN. Included in the mitotic CIN attractor are key components of mitotic checkpoint signaling²⁶, such as BUB1B, MAD2L1 (aka MAD2), CDC20, and TTK (aka MSP1). Also among the genes in the attractor is *MKI67* (aka *Ki-67*), which has been widely used as a proliferation rate marker in cancer.

Among transcription factors, we found *MYBL2* (aka *B-Myb*) and *FOXMI* to be strongly associated with the attractor. They are already known to be sequentially recruited to promote late cell cycle gene expression²⁷ to prepare for mitosis.

Inactivation of the retinoblastoma (RB) tumor suppressor promotes CIN²⁸ and the expression of the attractor signature. Indeed, a similar expression of a “proliferation gene cluster”²⁹ was found strongly associated with the human papillomavirus E7 oncogene, which abrogates RB protein function and activates E2F-regulated genes. Consistently, many among the genes of the attractor correspond to E2F pathway genes controlling cell division or proliferation. Among the E2F transcription factors, we found that E2F8 and E2F7 are most strongly associated with the attractor.

A lymphocyte-specific attractor

This attractor consists mainly of lymphocyte-specific genes with prominent presence of *CD53*, *PTPRC*, *LAPTM5*, *DOCK2* and *LCP2*. It is strongly associated³⁰ with the expression of microRNA miR-142 as well as with particular hypermethylated and hypomethylated gene signatures, which we reconfirmed to be consistent methylation attractors in cancer methylation data with our methodology. There is also significant overlap between the sets of hypomethylated and overexpressed genes, suggesting that their expression is triggered by hypomethylation. Gene set enrichment analysis reveals that the attractor is found enriched in genes known to be preferentially expressed in differentiation into lymphocytes³¹ and is also found occasionally upregulated in various cancers. Table 3 provides a listing of the top 100 genes of the attractor based on their average mutual information with their corresponding attractor metagenes.

Chr8q24.3 amplicon attractor

Amplification in chr8q24 is often associated with cancer because of the presence of the *MYC* (aka *c-Myc*) oncogene at location 8q24.21. Indeed, *MYC* is one of 157 genes in “amplicon 8q23-q24” previously identified³² in an extensive study of the breast cancer “amplicome” derived from 191 samples.

We found, however, that the core of the amplified genes occurs at location 8q24.3 and this is, in fact, our most prominent multi-cancer amplicon attractor. The main core gene of the attractor appears to be *PUF60* (aka *FIR*). Other consistently present top genes are *EXOSC4*, *CYCI*, *SHARPIN*, *HSF1*, *GPR172A*. It is known that *PUF60* can repress *c-Myc* via its far upstream element (*FUSE*), although a particular isoform was found to have the opposite effect³³. The other genes may also play important roles. For example, *HSF1* (heat shock transcription factor 1) has been associated with cancer in various ways³⁴. It was found³⁵ that *HSF1* can induce genomic instability through direct interaction with *CDC20*, a key gene of the mitotic CIN attractor mentioned above (listed in Table 2). Furthermore, *HSF1* was found³⁶ required for the cell transformation and tumorigenesis induced by the *ERBB2* (aka *HER2*) oncogene (see subsequent discussion of *HER2* amplicon) responsible for aggressive breast tumors.

The top ten genes of the chr8q24.3 attractor, ranked by the average of the highest five values of mutual information, are shown in Table 4. Interestingly, one of our identified general attractor corresponds to an aneuploidy involving a whole arm amplification of chr8q, which is occasionally present in multiple cancer types, and this 8q amplification is the most prominent such aneuploidy attractor among all chromosomes.

Chr17q12 HER2 amplicon attractor

This amplicon is prominent in breast cancer³⁷ and we also found it present in some samples of ovarian cancer, but not as much in colon cancer. So we initially used the four data sets of breast and ovarian cancer for deriving the attractor. We found that *ERBB2* (aka *HER2*), *STAR3*, *GRB7* and *PGAP3* were the top-ranked genes, consistent with their known presence in the amplicon. We also found that gene *MIEN1* (aka *C17orf37*) was very highly ranked in the two data sets in which its probe set was present. *MIEN1* has recently been identified as an important gene within the 17q12 amplicon in various cancers including prostate cancer³⁸. Therefore, we augmented the choice of datasets to the following seven, of which *MIEN1* is included in five: breast GSE2034, breast GSE32646, breast GSE36771, breast TCGA, ovarian GSE9891, ovarian GSE26193, ovarian TCGA. Table 4 shows the top ten genes ranked by the average of the top five scores of mutual information in the seven datasets for each gene. The results suggest that the above-mentioned five genes, including *MIEN1*, are consistently strongly co-expressed, and therefore are likely “driver” genes in the amplicon.

In addition to the narrow *HER2* amplicon, it is known that sometimes a large amplicon extends to more than a million bases containing both *HER2* as well as *TOP2A* (one of the genes of the mitotic CIN attractor) at 17q21³⁹. We have observed that *TOP2A* indeed appears among the top 50 genes in terms of its association with the attractor in breast cancer. *HER2/TOP2A* co-amplification has been linked with better clinical response to therapy.

Estrogen receptor breast cancer attractor

We found this attractor clearly present only in breast cancer, and therefore we derived it using six breast cancer data sets (GSE2034, GSE3494, GSE31448, GSE32646, GSE36771, breast TCGA). Table 5 shows the top 50 genes ranked by the average mutual information in these datasets, revealing that genes *CA12*, *AGR2*, *GATA3*, *FOXA1*, *MLPH* and *TBC1D9* are strongly co-expressed with the estrogen receptor *ESR1* in the attractor.

Using attractor metagenes as proxies of biomolecular events

A biomolecular event, whether it is present in multiple cancer types or it is cancer specific, can be represented by a “consensus attractor metagene” after analyzing multiple datasets. To generate such consensus attractors, we rank individual genes in terms of their average mutual information (Online Methods) with the corresponding attractor metagenes across all datasets.

For example, Figure 1 clarifies the previously reported⁴⁰ observation that breast tumors with high chromosomal instability are predominantly of the estrogen receptor negative phenotype. The scatter plots of the mitotic CIN and estrogen receptor metagenes shown in Figure 1, however, demonstrate that the nature of the association is that ER negative tumors have high mitotic chromosomal instability (or equivalently that low chromosomal instability implies that the tumor is ER positive), but the reverse relationship is not as clear.

DISCUSSION

Gene expression analysis has resulted in several cancer types being further classified into subtypes labeled, e.g. as “mesenchymal” or “proliferative.” Such characterizations, however, may sometimes simply reflect the presence of the mesenchymal transition attractor or the mitotic chromosomal instability attractor, respectively, in some of the analyzed samples. Similar subtype characterizations across cancer types often share several common genes, but the consistency of these similarities has not been significantly high.

In contrast, using an unconstrained algorithm independent of subtype classification or dimensionality reduction, we identified several attractors exhibiting remarkable consistency across many cancer types, suggesting that each of them represents a precise biological phenomenon present in multiple cancers.

We found that the mesenchymal transition attractor is significantly present only in samples whose stage designation has exceeded a threshold, but not in all of such samples. Similarly, we found that the mitotic chromosomal instability attractor is significantly present only in samples whose grade designation has exceeded a threshold, but not in all of them. On the other hand, the absence of the mesenchymal transition attractor in a profiled high-stage sample (or the absence of the mitotic chromosomal instability attractor in a profiled high-grade sample) does not necessarily mean that the attractor is not present in other locations of the same tumor. Indeed, it is increasingly appreciated⁴¹ that tumors are highly heterogeneous. Therefore it is possible for the same tumor to contain components, in which, e.g., some are migratory having undergone mesenchymal transition, some other ones are highly proliferative, etc. If so, attempts for subtype classification based on one particular site in a sample may be confusing.

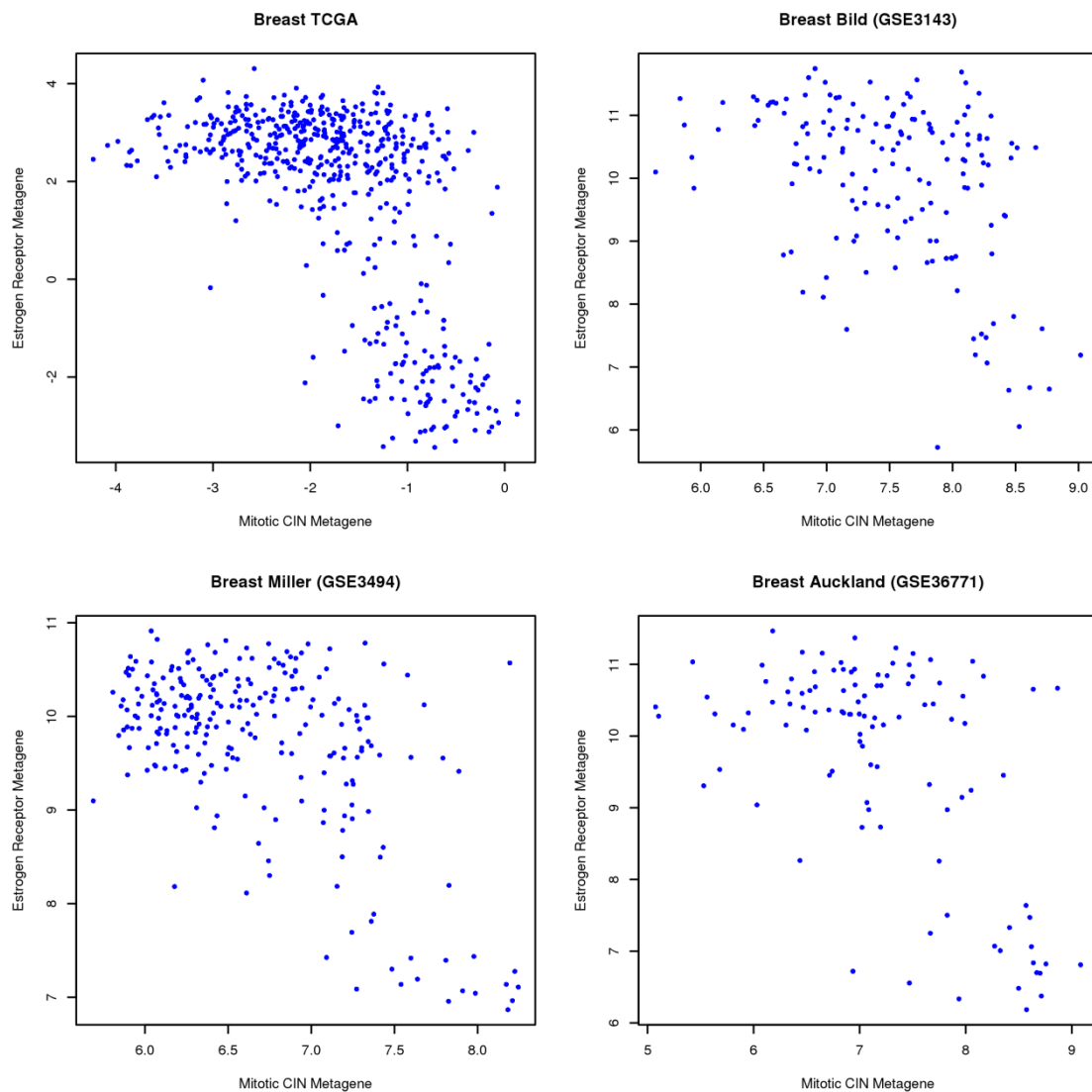
Similarly, existing molecular marker products make use of multigene assays that have been derived from phenotypic associations in particular cancer types. For breast cancer, biomarkers such as Oncotype DX⁴² and Mammaprint⁴³ contain several genes highly ranked in our attractors. For example, most of the genes used for the Oncotype DX breast cancer recurrence score directly converge to one of our identified attractors: *MMP11* to the mesenchymal transition attractor; *MKI67* (aka *Ki-67*), *AURKA* (aka *STK15*), *BIRC5* (aka *Survivin*), *CCNB1*, and *MYBL2* to the mitotic CIN attractor; *CD68*

to the lymphocyte-specific attractor; *ERBB2* and *GRB7* to the HER2 amplicon attractor; and *ESR1*, *SCUBE2*, *PGR* to the estrogen receptor attractor.

We envision, instead, a “multidimensional” biomarker product that will be applicable to multiple cancer types. Each of the dimensions will correspond to a specific attractor detected from a sharp choice of the genes at its core, reflecting a precise biological attribute of cancer. For example, each relevant amplicon can be identified by the coordinate co-expression of the top few genes of the attractor without any need for sequencing, and each amplicon will correspond to another dimension. The collection of the independent results in many dimensions will provide a clearer diagnostic and prognostic image after cleanly distinguishing the contributions of each component. Even though molecular marker genes in existing products are often separated into groups that are related to our attractor designation, any improvement in diagnostic, prognostic, or predictive accuracy resulting from better such group designation and better choice of genes in each group would be highly desirable. We hope that the computational methodology of identifying the attractors of cancer, as presented here, will be valuable in that regard.

Figures

Figure 1: Scatter plots demonstrating the relationship between mitotic CIN attractor and estrogen receptor attractor in breast cancer. The two metagenes were defined to be “consensus attractors” after ranking individual genes in terms of their average mutual information with the corresponding attractor metagenes, across all datasets, and selecting the genes having average mutual information greater than 0.5. These criteria led to 47 genes in the consensus mitotic CIN attractor (the top 47 genes in Table 2), and *ESR1*, *CA12*, *AGR2*, *GATA3*, *FOXA1*, *MLPH* and *TBC1D9* (the top seven genes in Table 5) in the consensus estrogen receptor breast cancer attractor. These scatter plots reveal that ER-negative breast tumors have high mitotic chromosomal instability, but not necessarily vice versa.



Tables

Table 1: Top 100 genes of the mesenchymal transition attractor based on six datasets

Rank	Gene	Avg MI	Rank	Gene	Avg MI	Rank	Gene	Avg MI
1	<i>COL5A2</i>	0.814	34	<i>FN1</i>	0.545	67	<i>SPON2</i>	0.444
2	<i>VCAN</i>	0.776	35	<i>LRRC15</i>	0.534	68	<i>SPOCK1</i>	0.444
3	<i>SPARC</i>	0.767	36	<i>COL11A1</i>	0.529	69	<i>COL8A2</i>	0.441
4	<i>THBS2</i>	0.759	37	<i>ANTXR1</i>	0.529	70	<i>PDPN</i>	0.437
5	<i>FBN1</i>	0.750	38	<i>RAB31</i>	0.527	71	<i>LHFP</i>	0.436
6	<i>COL1A2</i>	0.750	39	<i>THY1</i>	0.519	72	<i>GREM1</i>	0.436
7	<i>COL5A1</i>	0.747	40	<i>NNMT</i>	0.518	73	<i>GFPT2</i>	0.436
8	<i>FAP</i>	0.734	41	<i>SULF1</i>	0.506	74	<i>TGFB111</i>	0.435
9	<i>AEBP1</i>	0.712	42	<i>LOXL1</i>	0.502	75	<i>C1S</i>	0.433
10	<i>CTSK</i>	0.709	43	<i>PRRX1</i>	0.502	76	<i>EDNRA</i>	0.433
11	<i>COL3A1</i>	0.688	44	<i>COL10A1</i>	0.499	77	<i>GAS1</i>	0.431
12	<i>COL1A1</i>	0.684	45	<i>MXRA8</i>	0.494	78	<i>NOX4</i>	0.431
13	<i>SERPINF1</i>	0.674	46	<i>WISP1</i>	0.484	79	<i>FBLN2</i>	0.429
14	<i>COL6A3</i>	0.670	47	<i>RCN3</i>	0.483	80	<i>TCF4</i>	0.428
15	<i>CDH11</i>	0.663	48	<i>TNFAIP6</i>	0.481	81	<i>NUAK1</i>	0.428
16	<i>GLT8D2</i>	0.658	49	<i>ECM2</i>	0.480	82	<i>ADAMTS2</i>	0.422
17	<i>MMP2</i>	0.654	50	<i>HTRA1</i>	0.480	83	<i>NDN</i>	0.419
18	<i>LUM</i>	0.654	51	<i>EFEMP2</i>	0.478	84	<i>DPYSL3</i>	0.418
19	<i>DCN</i>	0.650	52	<i>MXRA5</i>	0.474	85	<i>LAMA4</i>	0.418
20	<i>POSTN</i>	0.631	53	<i>ACTA2</i>	0.472	86	<i>MFAP5</i>	0.418
21	<i>ADAM12</i>	0.614	54	<i>LOX</i>	0.470	87	<i>LGALS1</i>	0.417
22	<i>COL6A2</i>	0.609	55	<i>ITGBL1</i>	0.466	88	<i>PLAU</i>	0.417
23	<i>OLFML2B</i>	0.607	56	<i>PMP22</i>	0.465	89	<i>DSE</i>	0.417
24	<i>INHBA</i>	0.601	57	<i>PTRF</i>	0.463	90	<i>COLEC12</i>	0.416
25	<i>FSTL1</i>	0.600	58	<i>CALD1</i>	0.460	91	<i>DACT1</i>	0.415
26	<i>SNAI2</i>	0.577	59	<i>HEG1</i>	0.458	92	<i>CD248</i>	0.402
27	<i>CRISPLD2</i>	0.574	60	<i>NID2</i>	0.455	93	<i>COL6A1</i>	0.402
28	<i>PDGFRB</i>	0.567	61	<i>TAGLN</i>	0.455	94	<i>RARRES2</i>	0.401
29	<i>PCOLCE</i>	0.566	62	<i>SFRP4</i>	0.451	95	<i>JAM3</i>	0.398
30	<i>BGN</i>	0.566	63	<i>PALLD</i>	0.450	96	<i>SGCD</i>	0.397
31	<i>ANGPTL2</i>	0.555	64	<i>OLFML1</i>	0.448	97	<i>EMILIN1</i>	0.394
32	<i>COPZ2</i>	0.553	65	<i>FILIP1L</i>	0.447	98	<i>ZFPM2</i>	0.394
33	<i>ASPN</i>	0.547	66	<i>TIMP3</i>	0.445	99	<i>IGFBP7</i>	0.394
						100	<i>ZEB1</i>	0.394

Table 2: Top 100 genes of the mitotic CIN attractor based on six datasets

Rank	Gene	Avg MI	Rank	Gene	Avg MI	Rank	Gene	Avg MI
1	<i>CENPA</i>	0.727	34	<i>EXO1</i>	0.539	67	<i>ESPL1</i>	0.448
2	<i>MELK</i>	0.679	35	<i>AURKA</i>	0.538	68	<i>FAM64A</i>	0.442
3	<i>KIF2C</i>	0.667	36	<i>CDKN3</i>	0.538	69	<i>SPAG5</i>	0.436
4	<i>BUB1</i>	0.664	37	<i>DEPDC1</i>	0.536	70	<i>MYBL2</i>	0.436
5	<i>KIF4A</i>	0.660	38	<i>RRM2</i>	0.535	71	<i>EZH2</i>	0.432
6	<i>CCNB2</i>	0.659	39	<i>CDCA8</i>	0.535	72	<i>SMC4</i>	0.432
7	<i>KIF20A</i>	0.657	40	<i>SPC25</i>	0.534	73	<i>C12orf48</i>	0.431
8	<i>CCNA2</i>	0.652	41	<i>KIF18A</i>	0.528	74	<i>TACC3</i>	0.429
9	<i>TTK</i>	0.649	42	<i>PLK1</i>	0.508	75	<i>ASF1B</i>	0.427
10	<i>CEP55</i>	0.638	43	<i>HMMR</i>	0.506	76	<i>ERCC6L</i>	0.424
11	<i>CCNB1</i>	0.637	44	<i>TOP2A</i>	0.505	77	<i>TK1</i>	0.422
12	<i>CDC20</i>	0.623	45	<i>CENPF</i>	0.504	78	<i>TROAP</i>	0.421
13	<i>NCAPH</i>	0.622	46	<i>ZWINT</i>	0.502	79	<i>RFC4</i>	0.420
14	<i>BUB1B</i>	0.613	47	<i>RAD51AP1</i>	0.502	80	<i>PLK4</i>	0.420
15	<i>KIF23</i>	0.602	48	<i>CENPE</i>	0.498	81	<i>MCM6</i>	0.416
16	<i>KIF11</i>	0.592	49	<i>E2F8</i>	0.496	82	<i>KIAA0101</i>	0.415
17	<i>BIRC5</i>	0.588	50	<i>MKI67</i>	0.494	83	<i>GINS1</i>	0.408
18	<i>AURKB</i>	0.588	51	<i>CENPN</i>	0.491	84	<i>BLM</i>	0.406
19	<i>NUSAP1</i>	0.586	52	<i>CHEK1</i>	0.488	85	<i>CKS2</i>	0.402
20	<i>TPX2</i>	0.584	53	<i>MAD2L1</i>	0.487	86	<i>MCM2</i>	0.402
21	<i>RACGAP1</i>	0.583	54	<i>GTSE1</i>	0.477	87	<i>CENPI</i>	0.396
22	<i>PRC1</i>	0.582	55	<i>DTL</i>	0.475	88	<i>NCAPG2</i>	0.393
23	<i>ASPM</i>	0.581	56	<i>RAD51</i>	0.474	89	<i>STMN1</i>	0.392
24	<i>MCM10</i>	0.578	57	<i>SHCBP1</i>	0.468	90	<i>NEIL3</i>	0.389
25	<i>NEK2</i>	0.573	58	<i>TRIP13</i>	0.468	91	<i>ARHGAP11A</i>	0.387
26	<i>UBE2C</i>	0.569	59	<i>FBXO5</i>	0.466	92	<i>ATAD2</i>	0.384
27	<i>FOXM1</i>	0.563	60	<i>FANCI</i>	0.464	93	<i>CDC6</i>	0.383
28	<i>CDCA3</i>	0.560	61	<i>FEN1</i>	0.463	94	<i>CDC7</i>	0.378
29	<i>NDC80</i>	0.555	62	<i>CDC25C</i>	0.459	95	<i>CCDC99</i>	0.377
30	<i>STIL</i>	0.553	63	<i>ECT2</i>	0.459	96	<i>CKS1B</i>	0.375
31	<i>KIF15</i>	0.553	64	<i>RAD54L</i>	0.458	97	<i>RNASEH2A</i>	0.374
32	<i>KIF14</i>	0.542	65	<i>PBK</i>	0.456	98	<i>PSRC1</i>	0.373
33	<i>OIP5</i>	0.540	66	<i>KPNA2</i>	0.453	99	<i>DONSON</i>	0.371
						100	<i>CDC25A</i>	0.360

Table 3: Top 100 genes of the lymphocyte-specific attractor based on six datasets

Rank	Gene Symbol	Avg MI	Rank	Gene Symbol	Avg MI	Rank	Gene Symbol	Avg MI
1	<i>PTPRC</i>	0.782	34	<i>GPR65</i>	0.581	67	<i>NCKAP1L</i>	0.482
2	<i>CD53</i>	0.768	35	<i>CD52</i>	0.580	68	<i>CD247</i>	0.481
3	<i>LCP2</i>	0.739	36	<i>GIMAP6</i>	0.579	69	<i>GZMK</i>	0.480
4	<i>LAPTM5</i>	0.707	37	<i>SLAMF8</i>	0.578	70	<i>SELL</i>	0.479
5	<i>DOCK2</i>	0.699	38	<i>WIPF1</i>	0.576	71	<i>LY86</i>	0.479
6	<i>IL10RA</i>	0.699	39	<i>MS4A4A</i>	0.574	72	<i>CCR2</i>	0.479
7	<i>CYBB</i>	0.698	40	<i>ARHGAP15</i>	0.573	73	<i>ITGAM</i>	0.478
8	<i>CD48</i>	0.691	41	<i>CLEC4A</i>	0.566	74	<i>CORO1A</i>	0.477
9	<i>ITGB2</i>	0.679	42	<i>CCL5</i>	0.557	75	<i>LILRB1</i>	0.473
10	<i>EVI2B</i>	0.675	43	<i>LST1</i>	0.557	76	<i>CD74</i>	0.473
11	<i>MS4A6A</i>	0.673	44	<i>CD3D</i>	0.544	77	<i>GPR171</i>	0.471
12	<i>TFEC</i>	0.660	45	<i>FGL2</i>	0.539	78	<i>HLA-DMB</i>	0.469
13	<i>SLA</i>	0.657	46	<i>FCGR2B</i>	0.532	79	<i>ARHGAP25</i>	0.468
14	<i>SAMSN1</i>	0.652	47	<i>MYO1F</i>	0.530	80	<i>NCF4</i>	0.468
15	<i>PLEK</i>	0.649	48	<i>CD163</i>	0.524	81	<i>CSF2RB</i>	0.467
16	<i>GIMAP4</i>	0.647	49	<i>CLEC7A</i>	0.521	82	<i>IL7R</i>	0.464
17	<i>GMFG</i>	0.647	50	<i>CCR1</i>	0.517	83	<i>BTK</i>	0.463
18	<i>EVI2A</i>	0.638	51	<i>HLA-DPA1</i>	0.516	84	<i>CD69</i>	0.463
19	<i>SRGN</i>	0.637	52	<i>NCF2</i>	0.516	85	<i>HLA-DPB1</i>	0.455
20	<i>AIF1</i>	0.636	53	<i>RNASE6</i>	0.515	86	<i>ITK</i>	0.454
21	<i>LAIR1</i>	0.627	54	<i>CD14</i>	0.515	87	<i>TLR1</i>	0.454
22	<i>FYB</i>	0.625	55	<i>CD4</i>	0.510	88	<i>HLA-DMA</i>	0.451
23	<i>FCER1G</i>	0.623	56	<i>CD84</i>	0.505	89	<i>LILRB4</i>	0.449
24	<i>CD86</i>	0.621	57	<i>NKG7</i>	0.504	90	<i>IL2RG</i>	0.447
25	<i>C3AR1</i>	0.611	58	<i>C1QA</i>	0.503	91	<i>TLR2</i>	0.446
26	<i>C1QB</i>	0.609	59	<i>TRAF3IP3</i>	0.494	92	<i>ALOX5AP</i>	0.444
27	<i>CD2</i>	0.606	60	<i>TYROBP</i>	0.492	93	<i>IFI30</i>	0.443
28	<i>HCLS1</i>	0.599	61	<i>LPXN</i>	0.492	94	<i>IRF8</i>	0.443
29	<i>HCK</i>	0.592	62	<i>IL2RB</i>	0.490	95	<i>ITGAL</i>	0.441
30	<i>MNDA</i>	0.588	63	<i>IGSF6</i>	0.488	96	<i>TLR8</i>	0.438
31	<i>CD37</i>	0.587	64	<i>CD300A</i>	0.488	97	<i>PVRIG</i>	0.437
32	<i>CCR5</i>	0.585	65	<i>SELPLG</i>	0.488	98	<i>FLI1</i>	0.436
33	<i>LY96</i>	0.584	66	<i>FCGR2A</i>	0.486	99	<i>HLA-DRA</i>	0.434
						100	<i>LCK</i>	0.433

Table 4: List of top ten genes in the chr8q24.3 and HER2 amplicons

chr8q24.3		HER2	
Gene	Avg MI	Gene	Avg MI
<i>PUF60</i>	0.694	<i>ERBB2</i>	0.729
<i>EXOSC4</i>	0.655	<i>STARD3</i>	0.710
<i>SHARPIN</i>	0.635	<i>GRB7</i>	0.641
<i>GPR172A</i>	0.620	<i>PGAP3</i>	0.636
<i>CYC1</i>	0.594	<i>MIEN1</i>	0.615
<i>HSF1</i>	0.571	<i>PSMD3</i>	0.494
<i>FBXL6</i>	0.567	<i>ORMDL3</i>	0.437
<i>PYCRL</i>	0.550	<i>GSDMB</i>	0.403
<i>GPAA1</i>	0.529	<i>MED24</i>	0.354
<i>SCRIB</i>	0.483	<i>PNMT</i>	0.310

Table 5: Top 50 genes of the estrogen receptor breast cancer attractor

Rank	Gene Symbol	Avg MI	Rank	Gene Symbol	Avg MI
1	<i>CA12</i>	0.596	26	<i>SLC44A4</i>	0.344
2	<i>AGR2</i>	0.567	27	<i>SLC7A8</i>	0.339
3	<i>GATA3</i>	0.553	28	<i>BCL11A</i>	0.338
4	<i>FOXA1</i>	0.551	29	<i>FBP1</i>	0.338
5	<i>MLPH</i>	0.521	30	<i>MAGED2</i>	0.336
6	<i>ESR1</i>	0.519	31	<i>SLC22A5</i>	0.335
7	<i>TBC1D9</i>	0.502	32	<i>GREB1</i>	0.333
8	<i>ANXA9</i>	0.443	33	<i>EN1</i>	0.333
9	<i>DNALI1</i>	0.424	34	<i>PSAT1</i>	0.330
10	<i>SCUBE2</i>	0.423	35	<i>FOXC1</i>	0.329
11	<i>NAT1</i>	0.422	36	<i>C6orf211</i>	0.325
12	<i>XBP1</i>	0.421	37	<i>C6orf97</i>	0.324
13	<i>TFF3</i>	0.407	38	<i>VGLL1</i>	0.321
14	<i>ABAT</i>	0.405	39	<i>CLSTN2</i>	0.316
15	<i>GFRA1</i>	0.397	40	<i>IL6ST</i>	0.309
16	<i>DNAJC12</i>	0.395	41	<i>CELSR1</i>	0.304
17	<i>TFF1</i>	0.392	42	<i>TSPAN13</i>	0.302
18	<i>SLC39A6</i>	0.391	43	<i>EVL</i>	0.302
19	<i>SPDEF</i>	0.382	44	<i>ACADSB</i>	0.300
20	<i>ERBB4</i>	0.378	45	<i>SIDT1</i>	0.298
21	<i>THSD4</i>	0.374	46	<i>PGR</i>	0.296
22	<i>MAPT</i>	0.354	47	<i>C9orf116</i>	0.296
23	<i>AR</i>	0.349	48	<i>C14orf45</i>	0.288
24	<i>DACH1</i>	0.348	49	<i>INPP4B</i>	0.287
25	<i>MYB</i>	0.348	50	<i>AFF3</i>	0.287

ONLINE METHODS

General attractor finding algorithm

We chose the association measure $J(G_i, G_j)$ between genes to be a power function with exponent a of a normalized estimated information theoretic measure of the mutual information⁴⁴ $I(G_i, G_j)$ with minimum value 0 and maximum value 1 (see “Mutual information estimation” below; more sophisticated related association measures⁴⁵ can also be used, but computational complexity will be prohibitive). In other words, $J(G_i, G_j) = I^a(G_i, G_j)$, in which the exponent a can be any nonnegative number. Each iteration defines a new metagene in which the weight w_i for gene G_i is equal to $w_i = J(G_i, M)$, where M is the immediately preceding metagene. The process is repeated until the magnitude of the difference between two consecutive weight vectors is less than a threshold, which we chose to be equal to 10^{-7} .

At one extreme, if a is sufficiently large then each of the seeds will create its own single-gene attractor because all other genes will always have near-zero weights. In that case, the total number of attractors will be equal to the number of genes. At the other extreme, if a is zero then all weights will remain equal to each other representing the average of all genes, so there will only be one attractor. The higher the value of a , the “sharper” (more focused on its top gene) each attractor will be and the higher the total number of attractors will be. As the value of a is gradually decreased, the attractor from a particular seed will transform itself, occasionally in a discontinuous manner, thus providing insight into potential related biological mechanisms.

We empirically found that an appropriate choice of a (in the sense of revealing single biomolecular events of co-expressed genes) for general attractors is around 5, in which case there will typically be approximately 50 to 150 resulting attractors, each resulting from many attractee genes. An alternative to the power function can be a sigmoid function with varying steepness, but we found that the consistency of the resulting attractors was worse in that case.

An attractor metagene can also be interpreted as a set of the top genes of the attractor that includes only the genes that are significantly associated with the attractor. One empirical choice includes the genes whose mutual information (or the z-score thereof) with the attractor metagene exceeds a threshold. In fact, the attractor finding algorithm itself can be designed to discover attractor gene sets without assigning weights to genes. In that case, metagenes are defined as simple averages of the genes in a set, and each iteration leads to a new gene set consisting of the new set of top-ranked genes in terms of their association with the previous metagene (gene set sizes can be constant or adaptively changing). This method, however, has the disadvantage of occasionally leading to multiple overlapping attractors.

Identified attractors can be ranked in various ways. The “strength of an attractor” can be defined as the mutual information between the n^{th} top gene of the attractor and the attractor metagene. Indeed, if this measure is high, this implies that at

least the top n genes of the attractor are strongly co-expressed. We selected $n = 50$ as a reasonable choice, not too large, but sufficiently so to represent a real complex biological phenomenon of co-expression of at least 50 genes. For amplicons, $n = 5$ is sufficient to ensure that the oncogenes are included in the co-expression). We use these choices when referring to the strength of an attractor.

The top genes of many among the found attractors are genomically localized. In that case the biomolecular event that they represent is often the presence of a particular copy number variation. In the cancer datasets that we tried, this phenomenon almost always corresponds to a local amplification event known as an amplicon. We therefore also devised a related amplicon-finding algorithm, custom-designed to identify localized amplicon-representing attractor metagenes, described below.

Genomically localized attractor finding algorithm

To identify genomically localized attractors – almost always amplicons – we use the same algorithm but for each seed gene we restrict the set of candidate attractor genes to only include those in the local genomic neighbourhood of the gene, and we optimize the exponent a so that the strength of the attractor is maximized. Specifically, we sort the genes in each chromosome in terms of their genomic location and we only consider the genes within a window of size 51, i.e., with 25 genes on each side of the seed gene. We further optimize the choice of the exponent a for each seed, by allowing a to range from 1.0 to 6.0 with step size of 0.5 and selecting the attractor with the highest strength.

Because the set of allowed genes is different for each seed, the attractors will be different from each other, but “neighbouring” attractors will usually be very similar to each other. Therefore, following exhaustive attractor finding from each seed gene in a chromosome, we apply a filtering algorithm to only select the highest-strength attractor in each local genomic region, as follows: For each attractor, we rank all the genes in terms of their mutual information with the corresponding attractor metagene and we define the range of the attractor to be the chromosomal range of its top 15 genes. If there is any other attractor with overlapping range and higher strength, then the former attractor is filtered out. This filtering is done in parallel, so elimination of attractors occurs simultaneously.

Mutual information estimation

Assuming that the continuous expression levels of two genes G_1 and G_2 are governed by a joint probability density p_{12} with corresponding marginals p_1 and p_2 , the mutual information $I(G_1, G_2)$ is defined as the expected value of $\log(p_{12}/p_1p_2)$. It is a non-negative quantity representing the information that each one of the variables provides about the other. The pairwise mutual information has successfully been used as a general measure of the correlation between two random variables. We compute mutual information with a spline-based estimator⁴⁶ using six bins in each dimension. This method divides the observation space into equally spaced bins and blurs the boundaries between the bins with spline basis functions using third-order B-splines. We further

normalize the estimated mutual information by dividing by the maximum of the estimated $I(G_1, G_2)$ and $I(G_1, G_2)$, so the maximum possible value of $I(G_1, G_2)$ is 1.

Pre-processing gene expression datasets

We used Level 3 data when directly available, and imputed missing values using a k-nearest-neighbour algorithm with $k = 10$, as implemented in R⁴⁷. We normalized the other datasets on the Affymetrix platform using the RMA algorithm as implemented in the *affy* package in Bioconductor⁴⁸. To avoid biasing attractor convergence with multiple correlated probe sets of the same gene, we summarized the probe set-level expression values into the gene-level expression values by taking the mean of the expression values of probe sets for the same genes. We used the annotations for the probe sets given in the *jetset* package⁴⁹.

To investigate the associations between the attractor metagene expression and the tumor stage and grade, we used the following annotated gene expression datasets. For stage association: Breast (GSE3893), TCGA Ovarian, Colon (GSE14333). For grade association: Breast (GSE3494), TCGA Ovarian, Bladder (GSE13507). For Breast GSE3494 we used only the samples profiled by U133A arrays. For Breast GSE3893 we combined two platforms by taking the intersections of the probes in the U133A and the U133Plus 2.0 arrays. For datasets profiled by Affymetrix platforms all the datasets were normalized using the RMA algorithm. For Bladder GSE13507 normalization was done as provided in the GEO.

P value evaluation

P values for gene set enrichment were evaluated with the cumulative hypergeometric distribution using the total number of genes in each dataset.

1. Nevins, J.R. & Potti, A. Mining gene expression profiles: expression signatures as cancer phenotypes. *Nat Rev Genet* **8**, 601-609 (2007).
2. Collisson, E.A. et al. Subtypes of pancreatic ductal adenocarcinoma and their differing responses to therapy. *Nat Med* **17**, 500-503 (2011).
3. Verhaak, R.G. et al. Integrated genomic analysis identifies clinically relevant subtypes of glioblastoma characterized by abnormalities in PDGFRA, IDH1, EGFR, and NF1. *Cancer Cell* **17**, 98-110 (2010).
4. Cancer Genome Atlas Research, N. Integrated genomic analyses of ovarian carcinoma. *Nature* **474**, 609-615 (2011).
5. Brunet, J.P., Tamayo, P., Golub, T.R. & Mesirov, J.P. Metagenes and molecular pattern discovery using matrix factorization. *Proc Natl Acad Sci U S A* **101**, 4164-4169 (2004).
6. Monti, S., Tamayo, P., Mesirov, J. & Golub, T. Consensus clustering: A resampling-based method for class discovery and visualization of gene expression microarray data. *Machine Learning* **52**, 91-118 (2003).
7. Segal, E., Friedman, N., Kaminski, N., Regev, A. & Koller, D. From signatures to models: understanding cancer using microarrays. *Nat Genet* **37 Suppl**, S38-45 (2005).
8. Whitfield, M.L., George, L.K., Grant, G.D. & Perou, C.M. Common markers of proliferation. *Nat Rev Cancer* **6**, 99-106 (2006).
9. Kim, H., Watkinson, J., Varadan, V. & Anastassiou, D. Multi-cancer computational analysis reveals invasion-associated variant of desmoplastic reaction involving INHBA, THBS2 and COL11A1. *BMC Med Genomics* **3**, 51 (2010).
10. Anastassiou, D. et al. Human cancer cells express Slug-based epithelial-mesenchymal transition gene expression signature obtained in vivo. *BMC Cancer* **11**, 529 (2011).
11. Cheng, W.Y., Kandel, J.J., Yamashiro, D.J., Canoll, P. & Anastassiou, D. A multi-cancer mesenchymal transition gene expression signature is associated with prolonged time to recurrence in glioblastoma. *PLoS One* **7**, e34705 (2012).
12. Farmer, P. et al. A stroma-related gene signature predicts resistance to neoadjuvant chemotherapy in breast cancer. *Nat Med* **15**, 68-74 (2009).
13. Mani, S.A. et al. The epithelial-mesenchymal transition generates cells with properties of stem cells. *Cell* **133**, 704-715 (2008).
14. Hay, E.D. An overview of epithelio-mesenchymal transformation. *Acta Anat (Basel)* **154**, 8-20 (1995).
15. Thiery, J.P. Epithelial-mesenchymal transitions in tumour progression. *Nat Rev Cancer* **2**, 442-454 (2002).
16. Kalluri, R. & Weinberg, R.A. The basics of epithelial-mesenchymal transition. *J Clin Invest* **119**, 1420-1428 (2009).
17. Hanahan, D. & Weinberg, R.A. Hallmarks of cancer: the next generation. *Cell* **144**, 646-674 (2011).
18. Yin, G. et al. TWISTing stemness, inflammation and proliferation of epithelial ovarian cancer cells through MIR199A2/214. *Oncogene* **29**, 3545-3553 (2010).

19. Sotiriou, C. et al. Gene expression profiling in breast cancer: understanding the molecular basis of histologic grade to improve prognosis. *Journal of the National Cancer Institute* **98**, 262-272 (2006).
20. Carter, S.L., Eklund, A.C., Kohane, I.S., Harris, L.N. & Szallasi, Z. A signature of chromosomal instability inferred from gene expression profiles predicts clinical outcome in multiple human cancers. *Nat Genet* **38**, 1043-1048 (2006).
21. Schwartzman, J.M., Sotillo, R. & Benezra, R. Mitotic chromosomal instability and cancer: mouse modelling of the human disease. *Nat Rev Cancer* **10**, 102-115 (2010).
22. Yuen, K.W., Montpetit, B. & Hieter, P. The kinetochore and cancer: what's the connection? *Current opinion in cell biology* **17**, 576-582 (2005).
23. Amato, A., Schillaci, T., Lentini, L. & Di Leonardo, A. CENPA overexpression promotes genome instability in pRb-depleted human cells. *Mol Cancer* **8**, 119 (2009).
24. Sotillo, R., Schwartzman, J.M., Socci, N.D. & Benezra, R. Mad2-induced chromosome instability leads to lung tumour relapse after oncogene withdrawal. *Nature* **464**, 436-440 (2010).
25. Heidebrecht, H.J. et al. repp86: A human protein associated in the progression of mitosis. *Mol Cancer Res* **1**, 271-279 (2003).
26. Orr-Weaver, T.L. & Weinberg, R.A. A checkpoint on the road to cancer. *Nature* **392**, 223-224 (1998).
27. Sadasivam, S., Duan, S. & DeCaprio, J.A. The MuvB complex sequentially recruits B-Myb and FoxM1 to promote mitotic gene expression. *Genes & development* **26**, 474-489 (2012).
28. Manning, A.L. & Dyson, N.J. RB: mitotic implications of a tumour suppressor. *Nat Rev Cancer* **12**, 220-226 (2012).
29. Rosty, C. et al. Identification of a proliferation gene cluster associated with HPV E6/E7 expression level and viral DNA load in invasive cervical carcinoma. *Oncogene* **24**, 7094-7104 (2005).
30. Andreopoulos, B. & Anastassiou, D. Integrated Analysis Reveals hsa-miR-142 as a Representative of a Lymphocyte-Specific Gene Expression and Methylation Signature. *Cancer informatics* **11**, 61-75 (2012).
31. Lee, M.S., Hanspers, K., Barker, C.S., Korn, A.P. & McCune, J.M. Gene expression profiles during human CD4+ T cell differentiation. *International immunology* **16**, 1109-1124 (2004).
32. Nikolsky, Y. et al. Genome-wide functional synergy between amplified and mutated genes in human breast cancer. *Cancer Res* **68**, 9532-9540 (2008).
33. Matsushita, K. et al. An essential role of alternative splicing of c-myc suppressor FUSE-binding protein-interacting repressor in carcinogenesis. *Cancer Res* **66**, 1409-1417 (2006).
34. Dai, C., Whitesell, L., Rogers, A.B. & Lindquist, S. Heat shock factor 1 is a powerful multifaceted modifier of carcinogenesis. *Cell* **130**, 1005-1018 (2007).

35. Lee, Y.J. et al. A novel function for HSF1-induced mitotic exit failure and genomic instability through direct interaction between HSF1 and Cdc20. *Oncogene* **27**, 2999-3009 (2008).
36. Meng, L., Gabai, V.L. & Sherman, M.Y. Heat-shock transcription factor HSF1 has a critical role in human epidermal growth factor receptor-2-induced cellular transformation and tumorigenesis. *Oncogene* **29**, 5204-5213 (2010).
37. Theillet, C. What do we learn from HER2-positive breast cancer genomic profiles? *Breast Cancer Res* **12**, 107 (2010).
38. Dasgupta, S. et al. Novel gene C17orf37 in 17q12 amplicon promotes migration and invasion of prostate cancer cells. *Oncogene* **28**, 2860-2872 (2009).
39. Arriola, E. et al. Genomic analysis of the HER2/TOP2A amplicon in breast cancer and breast cancer cell lines. *Lab Invest* **88**, 491-503 (2008).
40. Birkbak, N.J. et al. Paradoxical relationship between chromosomal instability and survival outcome in cancer. *Cancer Res* **71**, 3447-3452 (2011).
41. Gerlinger, M. et al. Intratumor heterogeneity and branched evolution revealed by multiregion sequencing. *The New England journal of medicine* **366**, 883-892 (2012).
42. Paik, S. et al. A multigene assay to predict recurrence of tamoxifen-treated, node-negative breast cancer. *The New England journal of medicine* **351**, 2817-2826 (2004).
43. van 't Veer, L.J. et al. Gene expression profiling predicts clinical outcome of breast cancer. *Nature* **415**, 530-536 (2002).
44. Cover, T.M. & Thomas, J.A. Elements of information theory, Edn. 2nd. (Wiley-Interscience, Hoboken, N.J.; 2006).
45. Reshef, D.N. et al. Detecting novel associations in large data sets. *Science* **334**, 1518-1524 (2011).
46. Daub, C.O., Steuer, R., Selbig, J. & Kloska, S. Estimating mutual information using B-spline functions--an improved similarity measure for analysing gene expression data. *BMC Bioinformatics* **5**, 118 (2004).
47. Troyanskaya, O. et al. Missing value estimation methods for DNA microarrays. *Bioinformatics* **17**, 520-525 (2001).
48. Gautier, L., Cope, L., Bolstad, B.M. & Irizarry, R.A. affy--analysis of Affymetrix GeneChip data at the probe level. *Bioinformatics* **20**, 307-315 (2004).
49. Li, Q., Birkbak, N.J., Györfy, B., Szallasi, Z. & Eklund, A.C. Jetset: selecting the optimal microarray probe set to represent a gene. *BMC Bioinformatics* **12**, 474 (2011).